

Isospin violation in pion–kaon scattering^{#1}

Bastian Kubis^{#2}, Ulf-G. Meißner^{#3}

*Forschungszentrum Jülich, Institut für Kernphysik (Theorie)
D-52425 Jülich, Germany*

Abstract

We consider strong and electromagnetic isospin violation in near–threshold pion–kaon scattering. At tree level, such effects are small for all physical channels. We work out the complete one–loop corrections to the process $\pi^- K^+ \rightarrow \pi^0 K^0$. They come out rather small. We also show that the corresponding radiative cross section is highly suppressed at threshold.

Keywords: *pion–kaon scattering, electromagnetic corrections, chiral perturbation theory*

^{#1}Work supported in part by funds provided by the “Studienstiftung des deutschen Volkes”.

^{#2}E-mail: b.kubis@fz-juelich.de

^{#3}E-mail: Ulf-G.Meissner@fz-juelich.de

1 Introduction

The quark masses allow to consider various approximations to Quantum Chromodynamics (QCD). For the c , b , and t quarks, the masses are so large that an expansion in inverse powers of these masses can be performed systematically. This leads to the so-called heavy-quark effective field theory. On the other hand, to a good first approximation, one can consider the light quarks u , d , and s as massless. In that limit, the QCD Lagrangian exhibits a chiral symmetry which is, however, spontaneously broken as witnessed by the appearance of eight almost massless pseudoscalar Goldstone bosons, the pions, the kaons, and the eta. These would-be Goldstone bosons acquire their masses from the explicit symmetry breaking due to the quark mass term. Spontaneous as well as explicit symmetry violation can be explored systematically by means of chiral perturbation theory (ChPT), an effective field theory formulated in terms of the asymptotically observable fields. At low energies, the generating functional of QCD is characterized by two energy scales. One is the pion (kaon) decay constant in the chiral limit, denoted by F . Its non-vanishing value ($F \simeq 88$ MeV) is a necessary and sufficient condition for spontaneous symmetry breaking, much like the vacuum expectation value of the neutral Higgs boson signals the breaking of the electroweak symmetry. The second scale is given by the quark condensate, $B = |\langle 0|\bar{q}q|0\rangle|/F^2$. In the standard scenario of chiral symmetry breaking, $\langle 0|\bar{q}q|0\rangle \simeq (-225 \text{ MeV})^3$ so that $B \simeq 1.5 \text{ GeV} \gg F$. This leads e.g. to a very precise prediction for the S-wave $\pi\pi$ scattering lengths [1]. This scenario seems to be confirmed by recent Brookhaven data on $K_{\ell 4}$ decays [2] and will be further scrutinized when the ponium lifetime measurements performed at CERN [3] have been analyzed. For the three flavor sector, the situation is, however, less clear. Indeed, the observation that $m_s \simeq \Lambda_{\text{QCD}}$ has even led to investigations considering the strange quark as heavy [4, 5, 6]. Furthermore, there have been recent speculations that the structure of the QCD vacuum changes dramatically with increasing number of flavors, e.g. it could be possible that the condensate is sizeably suppressed in SU(3) as compared to SU(2) [7].

One of the cleanest processes to test our understanding of the symmetry breaking pattern in the presence of strange quarks is elastic pion-kaon (πK) scattering near threshold. This reaction is interesting for a variety of reasons. First, it is very similar to $\pi\pi$ scattering in the two-flavor sector but also different in that the quark mass difference $m_u - m_d$ can appear at leading order in the πK scattering amplitude. Second, there exist abundant data from inelastic processes which allow one to extract low-energy characteristics of the πK scattering amplitude by means of dispersion theory. The existing determinations of the S-wave scattering lengths are, however, plagued by large uncertainties, see e.g. [8]. For recent work on combining dispersion relations and chiral perturbation theory, see [9]. Third, the DIRAC collaboration intends to measure the lifetime of πK atoms at CERN [10] which gives direct access to the isovector S-wave scattering length. To also pin down the isoscalar S-wave scattering length, one would have to measure the $2P - 2S$ level shift, similar to what has been done for the pion-nucleon system at PSI [11]. The precise relation between the πK atom lifetime and the scattering length (the so-called modified Deser formula) can be worked out by means of an effective field theory for hadronic bound states (for the ponium case see e.g. [12, 13]).

To achieve the necessary accuracy in the πK system, it is mandatory to sharpen the existing one-loop predictions for the scattering lengths and range parameters [8, 14] by including isospin violation due to strong and electromagnetic effects. This is done here. First, we study isospin violation for the S-wave scattering lengths at tree level for all physical channels. This allows for a first estimate of such effects and is also interesting to compare directly to the $\pi\pi$ case. Then we focus on the one-loop strong and electromagnetic corrections to the relevant channel for πK atoms, $\pi^- K^+ \rightarrow \pi^0 K^0$, including also a complete treatment of soft photon radiation, $\pi^- K^+ \rightarrow \pi^0 K^0 \gamma$.

2 Lagrangians

In this section we discuss the strong and electromagnetic effective Lagrangians underlying our calculations. All the pieces have been discussed extensively elsewhere in the literature, so we will just present the terms needed for the following. The effective Lagrangian can be expanded at low energies according to

$$\mathcal{L}_{\text{eff}} = \mathcal{L}_{\text{str}}^{(2)} + \mathcal{L}_{\text{em}}^{(2)} + \mathcal{L}_{\text{str}}^{(4)} + \mathcal{L}_{\text{em}}^{(4)} + \dots, \quad (1)$$

where the superscripts (2), (4) refer to the chiral dimension and “str” and “em” denote the strong and electromagnetic terms, respectively. Chiral power counting for the strong sector attributes the chiral dimension q to all pseudo-Goldstone boson masses (M_π, M_K, M_η) as well as all momenta involved. This scheme is generalized to include electromagnetic terms by counting the electric charge e also as a quantity of order q , which is dictated by the requirement that a unique dimension be assigned to the covariant derivative (that includes the lowest order photon coupling). Therefore any term of the form $e^{2j} q^{2k} M_\pi^l M_K^m M_\eta^n$ with, e.g., $2j + 2k + l + m + n = 4$ is counted as fourth order.

The lowest-order Lagrangian is given by

$$\begin{aligned} \mathcal{L}^{(2)} &= -\frac{1}{4} F_{\mu\nu} F^{\mu\nu} - \frac{\lambda}{2} (\partial_\mu A^\mu)^2 \\ &+ \frac{F^2}{4} \langle D_\mu U^\dagger D^\mu U + \chi U^\dagger + \chi^\dagger U \rangle + C \langle QUQU^\dagger \rangle. \end{aligned} \quad (2)$$

Here, $\langle \dots \rangle$ denotes the trace in flavor space. $F_{\mu\nu} = \partial_\mu A_\nu - \partial_\nu A_\mu$ is the usual electromagnetic field strength tensor, λ refers to the gauge fixing parameter. All calculations were performed in the Feynman gauge, $\lambda = 1$. $U = \exp(i\Phi/F)$ collects the (pseudo-)Goldstone boson fields, the low-energy constant (LEC) F can be identified with a common meson decay constant in the chiral limit. $D_\mu U = \partial_\mu U - i[v_\mu, U] - i\{a_\mu, U\}$ defines the covariant derivative acting on U in the presence of external vector (v_μ) and axial vector (a_μ) currents. χ includes external scalar (s) and pseudoscalar (p) sources, $\chi = 2B(s + ip)$, where for our purposes, only the quark mass term in the source s is of relevance, $s = \mathcal{M} + \dots$, $\mathcal{M} = \text{diag}(m_u, m_d, m_s)$. The LEC B is linked to the quark condensate at leading order as already discussed in the introduction. Q is the quark charge matrix, $Q = e \text{diag}(2/3, -1/3, -1/3)$. The LEC C accompanying the last term in the Lagrangian eq. (2) can be calculated from the leading order electromagnetic pion mass difference, $M_{\pi^\pm}^2 - M_{\pi^0}^2 = 2Ze^2 F^2$ (neglecting a tiny strong

mass difference $\sim (m_u - m_d)^2$, where we have defined the convenient dimensionless constant $Z = C/F^4$. Using $F = F_\pi = 92.4$ MeV, one obtains $Z \approx 0.8$.

The fourth-order Lagrangian [15] contains the following ‘‘strong’’ terms which are needed for the amplitude describing the process $\pi^- K^+ \rightarrow \pi^0 K^0$ at one-loop level:

$$\begin{aligned} \mathcal{L}_{\text{str}}^{(4)} &= L_3 \langle D_\mu U^\dagger D^\mu U D_\nu U^\dagger D^\nu U \rangle + L_4 \langle D_\mu U^\dagger D^\mu U \rangle \langle \chi^\dagger U + \chi U^\dagger \rangle \\ &+ L_5 \langle D_\mu U^\dagger D^\mu U (\chi^\dagger U + U^\dagger \chi) \rangle + L_6 \langle \chi^\dagger U + \chi U^\dagger \rangle^2 \\ &+ L_7 \langle \chi^\dagger U - \chi U^\dagger \rangle^2 + L_8 \langle \chi^\dagger U \chi^\dagger U + \chi U^\dagger \chi U^\dagger \rangle . \end{aligned} \quad (3)$$

With regard to the analytic formulae given for the S-wave scattering length in app. A, we remark that only three of the LECs defined in eq. (3) play a role for this quantity at leading order in isospin violation. Terms depending on the Zweig rule suppressed constants L_4 and L_6 as well as on L_7 are of higher order in isospin breaking. In addition, the following electromagnetic counterterms given in [16] are needed:

$$\begin{aligned} \mathcal{L}_{\text{em}}^{(4)} &= K_1 F^2 \langle D_\mu U^\dagger D^\mu U \rangle \langle Q^2 \rangle + K_2 F^2 \langle D_\mu U^\dagger D^\mu U \rangle \langle QUQU^\dagger \rangle \\ &+ K_3 F^2 \left(\langle D_\mu U^\dagger QU \rangle \langle D^\mu U^\dagger QU \rangle + \langle D_\mu U QU^\dagger \rangle \langle D^\mu U QU^\dagger \rangle \right) \\ &+ K_4 F^2 \langle D_\mu U^\dagger QU \rangle \langle D^\mu U QU^\dagger \rangle + K_5 F^2 \langle (D_\mu U^\dagger D^\mu U + D_\mu U D^\mu U^\dagger) Q^2 \rangle \\ &+ K_6 F^2 \langle D_\mu U^\dagger D^\mu U QU^\dagger QU + D_\mu U D^\mu U^\dagger QUQU^\dagger \rangle + K_7 F^2 \langle \chi^\dagger U + \chi U^\dagger \rangle \langle Q^2 \rangle \\ &+ K_8 F^2 \langle \chi^\dagger U + \chi U^\dagger \rangle \langle QUQU^\dagger \rangle + K_9 F^2 \langle (\chi^\dagger U + U^\dagger \chi + \chi U^\dagger + U \chi^\dagger) Q^2 \rangle \\ &+ K_{10} F^2 \langle (\chi^\dagger U + U^\dagger \chi) QU^\dagger QU + (\chi U^\dagger + U \chi^\dagger) QUQU^\dagger \rangle \\ &+ K_{11} F^2 \langle (\chi^\dagger U - U^\dagger \chi) QU^\dagger QU + (\chi U^\dagger - U \chi^\dagger) QUQU^\dagger \rangle \\ &+ K_{15} F^4 \langle QUQU^\dagger \rangle^2 + K_{16} F^4 \langle QUQU^\dagger \rangle \langle Q^2 \rangle . \end{aligned} \quad (4)$$

Also the dependence on a few of these ($K_{7/8}$, $K_{15/16}$) cancels in the S-wave scattering length. One more term (proportional to K_{12} in [16]) that is needed in principle for the renormalization of the decay constants of charged mesons can be omitted in case one uses physical values for decay constants with electromagnetic effects already subtracted (see section 4.1).

For numerical evaluation, we use the central values and error estimates for the hadronic low-energy constants as given in [17]. For the electromagnetic ones, we use the estimates obtained via resonance saturation in [18], and add error bars of natural size ($\pm 1/16\pi^2$) uniformly.

3 Isospin violation at tree level

Pion-kaon scattering in the isospin limit can be described by two independent amplitudes $T^{1/2}$ and $T^{3/2}$, corresponding to isospin 1/2 and 3/2, respectively. It is sometimes convenient to combine these into isospin-even and -odd amplitudes T^\pm which are defined by

$$T_{\alpha\beta} = \delta_{\alpha\beta} T^+ + \frac{1}{2} [\tau_\alpha, \tau_\beta] T^- \quad (5)$$

(α, β refer to the isospin indices of the pions) and which can be related to the amplitudes of definite isospin via

$$3T^+ = T^{1/2} + 2T^{3/2}, \quad (6)$$

$$3T^- = T^{1/2} - T^{3/2}. \quad (7)$$

All these amplitudes can be expressed in terms of the usual Mandelstam variables s, t, u . They can be decomposed into partial waves $t_l^I(s)$ using

$$T^I(s, t) = 16\pi \sum_l (2l+1) t_l^I(s) P_l(z), \quad (8)$$

where $z = \cos\theta$ denotes the scattering angle in the center-of-mass system, and $P_l(z)$ are the Legendre polynomials. Close to threshold, one can parameterize the real parts of the partial wave amplitudes in terms of scattering lengths (a_l) and effective ranges (b_l),

$$\text{Re } t_l^I(s) = \frac{\sqrt{s}}{2} (|\mathbf{q}_{\text{in}}||\mathbf{q}_{\text{out}}|)^l \left\{ a_l^I + b_l^I |\mathbf{q}_{\text{in}}|^2 + \mathcal{O}(|\mathbf{q}_{\text{in}}|^4) \right\}, \quad (9)$$

where we have already accounted for the possibility of different masses of the incoming and outgoing particles and therefore for different incoming and outgoing center-of-mass momenta,

$$|\mathbf{q}_{\text{in}}| = \frac{\sqrt{(s - (M_K^{\text{in}} - M_\pi^{\text{in}})^2)(s - (M_K^{\text{in}} + M_\pi^{\text{in}})^2)}}{2\sqrt{s}}, \quad (10)$$

$$|\mathbf{q}_{\text{out}}| = \frac{\sqrt{(s - (M_K^{\text{out}} - M_\pi^{\text{out}})^2)(s - (M_K^{\text{out}} + M_\pi^{\text{out}})^2)}}{2\sqrt{s}}, \quad (11)$$

where $M_{\pi/K}^{\text{in/out}}$ refer to the physical masses of the incoming and outgoing pions and kaons, respectively. In the isospin limit, eq. (9) collapses to the usual definition. We note that the real part of a total amplitude at threshold (i.e. for $|\mathbf{q}_{\text{in}}| = 0$) is linked to the S-wave scattering length by

$$\text{Re } T_{\text{thr}}^I = 8\pi (M_K^{\text{in}} + M_\pi^{\text{in}}) a_0^I + \mathcal{O}(|\mathbf{q}_{\text{in}}|^2, |\mathbf{q}_{\text{in}}||\mathbf{q}_{\text{out}}|). \quad (12)$$

At tree level, the isospin-even and -odd pion-kaon scattering lengths are given by [19, 20]

$$a_0^+ = 0, \quad a_0^- = \frac{M_\pi M_K}{8\pi F_\pi^2 (M_\pi + M_K)} = 70.8 \times 10^{-3} / M_\pi. \quad (13)$$

The different physical pion-kaon channels receive corrections to their isospin symmetric scattering lengths when taking into account the mass differences as well as insertions stemming from the electromagnetic term in eq. (2). We collect the isospin breaking parameters as $\delta \in \{m_u - m_d, e^2\}$ and expand the corrections to the scattering lengths up to order δ . The following conventions were used:

- The isospin symmetry limit is defined according to e.g. [12], i.e. we express everything in terms of the *charged* meson masses M_{π^\pm} , M_{K^\pm} . Note that these are not exactly the natural choices from the point of view of a chiral analysis of the meson masses, in which case one would prefer to take the neutral pion mass as a reference (which is indeed done in [21]), as one has $M_{\pi^0}^2 = 2B\hat{m}$ (with $\hat{m} = \frac{1}{2}(m_u + m_d)$) to good accuracy, neglecting only tiny corrections of order $(m_u - m_d)^2$. However, one would consequently have to resolve to using a “non-physical” kaon mass $M_K^2 = B(\hat{m} + m_s) \approx 495$ MeV. Arguments *for* the use of the charged pion and kaon masses are the correct kinematics for the experimentally accessible channels (which use incoming charged particles), and the fact that the existing study of pion-kaon scattering in ChPT (in the isospin symmetry limit) [14] also employs these choices for numerical evaluation.
- As finally we want to evaluate isospin violating effects up to order e^2 and $m_u - m_d$, we can neglect the strong pion mass difference (of order $(m_u - m_d)^2$). Quark mass insertions can then, at leading order, be expressed by physical meson masses according to

$$\begin{aligned} \hat{m} &\rightarrow \frac{M_{\pi^0}^2}{2B}, & m_d - m_u &\rightarrow \frac{M_{K^0}^2 - M_{K^\pm}^2 + M_{\pi^\pm}^2 - M_{\pi^0}^2}{B}, \\ m_s &\rightarrow \frac{M_{K^\pm}^2 + M_{K^0}^2 - M_{\pi^\pm}^2}{2B}, & Z &\rightarrow \frac{M_{\pi^\pm}^2 - M_{\pi^0}^2}{2e^2 F_\pi^2}. \end{aligned} \quad (14)$$

- One important isospin breaking effect due to the light quark mass difference is $\pi^0\eta$ -mixing: the π^0 and η fields are given in terms of the SU(3) eigenstates ϕ_3 , ϕ_8 according to

$$\begin{pmatrix} \pi^0 \\ \eta \end{pmatrix} = \begin{pmatrix} \cos \epsilon & \sin \epsilon \\ -\sin \epsilon & \cos \epsilon \end{pmatrix} \begin{pmatrix} \phi_3 \\ \phi_8 \end{pmatrix}, \quad (15)$$

where the $\pi^0\eta$ mixing angle ϵ is given by

$$\epsilon = \frac{1}{2} \arctan \left(\frac{\sqrt{3} m_d - m_u}{2 m_s - \hat{m}} \right). \quad (16)$$

Replacing the quark masses by meson masses according to eq. (14), one finds the numerical value $\epsilon = 1.00 \times 10^{-2}$. We find it convenient to express all corrections due to the light quark mass difference in terms of this mixing angle ϵ , which is of course of order $m_u - m_d$.

Note finally that we only display scattering lengths for processes involving kaons of positive strangeness (K^+ , K^0) as the strong and electromagnetic interactions obey charge conjugation invariance, such that scattering lengths for all channels involving scattering of K^- or \bar{K}^0 can be obtained from those given below. We find:

$$\begin{aligned} a_0(\pi^+ K^+ \rightarrow \pi^+ K^+) &= a_0^{3/2} \left\{ 1 - \frac{2ZF_\pi^2}{M_\pi M_K} e^2 \right\} + \mathcal{O}(\delta^2) \\ &= a_0^{3/2} \{ 1 - 0.018 \} + \mathcal{O}(\delta^2), \end{aligned} \quad (17)$$

$$\begin{aligned}
a_0(\pi^+ K^0 \rightarrow \pi^+ K^0) &= (a_0^+ + a_0^-) \left\{ 1 + \frac{2(M_K - M_\pi)M_\pi}{\sqrt{3}M_K^2} \epsilon - \frac{Z M_\pi F_\pi^2}{M_K^2(M_K + M_\pi)} e^2 \right\} + \mathcal{O}(\delta^2) \\
&= (a_0^+ + a_0^-) \{1 + 0.002 - 0.001\} + \mathcal{O}(\delta^2), \tag{18}
\end{aligned}$$

$$\begin{aligned}
a_0(\pi^+ K^0 \rightarrow \pi^0 K^+) &= \sqrt{2} a_0^- \left\{ 1 - \frac{M_K^2 - 2M_K M_\pi + 2M_\pi^2}{\sqrt{3}M_K^2} \epsilon - \frac{Z(M_K^2 + M_\pi^2)F_\pi^2}{M_K^2 M_\pi(M_K + M_\pi)} e^2 \right\} \\
&\quad + \mathcal{O}(\delta^2) \\
&= \sqrt{2} a_0^- \{1 - 0.003 - 0.008\} + \mathcal{O}(\delta^2), \tag{19}
\end{aligned}$$

$$\begin{aligned}
a_0(\pi^0 K^+ \rightarrow \pi^0 K^+) &= a_0^+ - \frac{M_K^2}{4\sqrt{3}\pi F_\pi^2(M_K + M_\pi)} \epsilon + \mathcal{O}(\delta^2) \\
&= a_0^+ - 2.9 \times 10^{-3}/M_\pi + \mathcal{O}(\delta^2), \tag{20}
\end{aligned}$$

$$\begin{aligned}
a_0(\pi^- K^+ \rightarrow \pi^- K^+) &= (a_0^+ + a_0^-) \left\{ 1 + \frac{2ZF_\pi^2}{M_\pi M_K} e^2 \right\} + \mathcal{O}(\delta^2) \\
&= (a_0^+ + a_0^-) \{1 + 0.018\} + \mathcal{O}(\delta^2), \tag{21}
\end{aligned}$$

$$\begin{aligned}
a_0(\pi^- K^+ \rightarrow \pi^0 K^0) &= -\sqrt{2} a_0^- \left\{ 1 + \frac{\epsilon}{\sqrt{3}} + \frac{ZF_\pi^2}{M_\pi M_K} e^2 \right\} + \mathcal{O}(\delta^2) \\
&= -\sqrt{2} a_0^- \{1 + 0.006 + 0.009\} + \mathcal{O}(\delta^2), \tag{22}
\end{aligned}$$

$$\begin{aligned}
a_0(\pi^0 K^0 \rightarrow \pi^0 K^0) &= a_0^+ + \frac{M_K^2}{4\sqrt{3}\pi F_\pi^2(M_K + M_\pi)} \epsilon + \mathcal{O}(\delta^2) \\
&= a_0^+ + 2.9 \times 10^{-3}/M_\pi + \mathcal{O}(\delta^2), \tag{23}
\end{aligned}$$

$$\begin{aligned}
a_0(\pi^- K^0 \rightarrow \pi^- K^0) &= a_0^{3/2} \left\{ 1 + \frac{2(M_K - M_\pi)M_\pi}{\sqrt{3}M_K^2} \epsilon - \frac{ZM_\pi F_\pi^2}{M_K^2(M_K + M_\pi)} e^2 \right\} + \mathcal{O}(\delta^2) \\
&= a_0^{3/2} \{1 + 0.002 - 0.001\} + \mathcal{O}(\delta^2). \tag{24}
\end{aligned}$$

For the elastic charged channels, eqs. (17), (21), subtraction of the one-photon exchange Born term is required in order to arrive at the above results (see [22] for the comparable $\pi\pi$ case). These charged-particle Coulomb interactions in principle require a separate treatment tailored to scattering or bound-state problems. (For the $\pi\pi$ scattering problem, this is discussed e.g. in [23].) We remark that isospin violation effects can only be given in absolute size for those amplitudes which are (in the isospin limit) proportional to T^+ , as a_0^+ vanishes at tree level. The one-loop corrections to a_0^+ are rather large, $a_0^{+(4)} = 31.9 \times 10^{-3}/M_\pi$ [14], but still then the corrections displayed in eqs. (20), (23) amount to 10% effects. (The caveat is, of course, that isospin violating contributions at one-loop level might reduce the leading-order terms considerably.) In fact, this is neatly comparable to pion-nucleon scattering: as pointed out by Weinberg, the isoscalar πN amplitude vanishes at leading chiral order [19] and is therefore prone to display large isospin violation effects [24], which have indeed been confirmed in [25].

It is instructive to compare the results above also to the corresponding corrections calculated in [22] for $\pi\pi$ scattering. First of all, $m_u - m_d$ effects are suppressed in SU(2), such that the only isospin breaking corrections of interest in the $\pi\pi$ case are of electromagnetic origin. In contrast, strong isospin breaking appears at leading order in πK scattering and, as shown

above, is potentially of equal significance as the electromagnetic effects. On the other hand, the authors of [22] find corrections at tree level of the order of 6%, while the largest corrections given above are 1.8% (for the elastic charged meson channels). This is not due to a particular “smallness” of e.g. the electromagnetic contribution for πK scattering, but due to the fact that the (isospin conserving) S–wave scattering length is larger, $a_0(\pi K) \sim M_\pi M_K$ in contrast to $a_0(\pi\pi) \sim M_\pi^2$. As already hinted at in the introduction, processes with a conserved number of strange quarks (such as πK scattering) can also be studied in a chiral SU(2) theory in which Green’s functions are only expanded around the limit $m_u = m_d = 0$, while m_s is held fixed at its physical value. Consequently, only the pion is considered to be “light”, while the kaon is now a heavy particle and has to be treated in analogy to e.g. nucleons in ChPT, resulting in what one might call “heavy–kaon” ChPT [5, 6]. The πK Lagrangian then starts out at order q , as does the (isovector) πK scattering length (see again the analogy to πN scattering). In such a counting scheme, electromagnetic corrections to πK scattering lengths are therefore necessarily suppressed by one chiral order (as they scale like e^2), which sheds some light on why these corrections are smaller here than for $\pi\pi$ scattering.

We want to emphasize that it is in general impossible to arrive at the results above by assuming the dominance of certain “effects” for the violation of isospin symmetry, e.g. studying the implications of meson mass splittings or $\pi^0\eta$ mixing alone. From the point of view of ChPT, such a partial analysis is not very useful and can lead to strongly misleading results. In order to demonstrate this, we show such a decomposition (artificial though this really is) for the specific channel studied in more detail in the following chapter, $\pi^- K^+ \rightarrow \pi^0 K^0$. We distinguish “kinematical” effects (due to meson mass splittings, entering essentially via corrections to the values of u and t at threshold), “ $\pi^0\eta$ mixing” effects which modify the isospin symmetric amplitude by factors of $\sin \epsilon$ or $\cos \epsilon$, “quark mass insertions” for the four–meson vertex (which vanish in the isospin limit for the channel in question), and “electromagnetic (em) insertions” ($\sim Z$) for the four–meson vertex. The relative corrections can then be decomposed as follows:

$$\text{strong :} \quad \frac{\epsilon}{\sqrt{3}} = \frac{\epsilon}{\sqrt{3}} \left\{ \underbrace{1 - \frac{M_K}{M_\pi}}_{\text{kinematical}} + \underbrace{\frac{2M_K^2 + M_\pi^2}{3M_K M_\pi}}_{\pi^0\eta\text{-mixing}} + \underbrace{\frac{M_K^2 - M_\pi^2}{3M_K M_\pi}}_{\text{quark mass}} \right\}, \quad (25)$$

$$\text{electromagnetic :} \quad \frac{Ze^2 F_\pi^2}{M_K M_\pi} = \underbrace{\frac{Ze^2 F_\pi^2}{2M_K M_\pi}}_{\text{kinematical}} + \underbrace{\frac{Ze^2 F_\pi^2}{2M_K M_\pi}}_{\text{em insertions}}. \quad (26)$$

It is obvious from the above that for the strong isospin violating contributions, individual “effects” are much larger than the total sum.

4 $\pi^- K^+ \rightarrow \pi^0 K^0$ at one–loop level

4.1 S–wave scattering length up to fourth order

In this section, we work out the complete one–loop corrections including isospin breaking for the pion–kaon channel that is relevant for the lifetime of πK atoms, $\pi^- K^+ \rightarrow \pi^0 K^0$. At

this level, virtual photon loops play a role and enter the amplitude both via wave function renormalization and electromagnetic corrections to the (lowest order) strong vertex, see fig. 1. As is well known, the photon exchange diagram (a) in fig. 1 induces a pole at

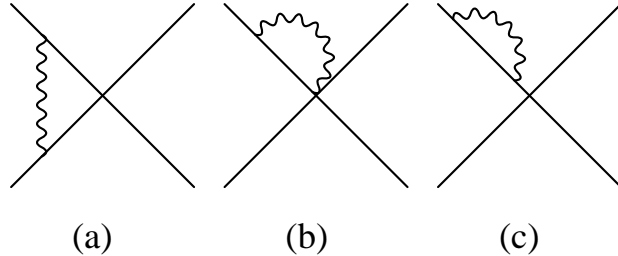


Figure 1: Virtual photon loop diagrams for $\pi^- K^+ \rightarrow \pi^0 K^0$. Crossed diagrams are not shown. Diagram (c) denotes effects entering the scattering amplitude via wave function renormalization of the incoming charged mesons.

threshold, the so-called Coulomb pole, which resides in the loop function $G^{\pi K \gamma}(s)$ discussed in detail in app. B. This Coulomb pole, however, can be calculated and subtracted from the amplitude unambiguously. The threshold expansion eq. (12) therefore has to be modified for $\pi^- K^+ \rightarrow \pi^0 K^0$ in the presence of virtual photons in order to sensibly define corrections to the S-wave scattering length:

$$\text{Re } T = \frac{e^2 \pi M_{K^\pm} M_{\pi^\pm} a_0^{(2)}}{|\mathbf{q}_{\text{in}}|} + 8\pi (M_{K^\pm} + M_{\pi^\pm}) a_0 + \mathcal{O}(|\mathbf{q}_{\text{in}}|), \quad (27)$$

where $a_0^{(2)}$ denotes the S-wave scattering length in its tree level approximation (given explicitly up to order δ in eq. (22)), and a_0 is the S-wave scattering length to be defined here, including all corrections.

A further problem occurs when including virtual photon loops: the amplitude becomes infrared divergent. We will give details on how to deal with these infrared divergences in the following section. For the moment we only note that these vanish at threshold and therefore do not affect the definition of the S-wave scattering length as given in eq. (27).

Analytic formulae for the S-wave scattering length at one-loop accuracy are given in app. A. In order to arrive at these, the following effects were taken into account, as well as the following conventions were used in addition to those already mentioned in the previous section:

- In order to have a strong check on the scattering amplitude, we have checked the cancellation of divergences in the *exact* expressions, i.e. without any expansion in ϵ and e^2 . For this purpose, we have used the β -functions for the various counterterms as given in [15, 16].
- For quark mass insertions at tree level replaced by meson masses according to eq. (14), the renormalization of these meson masses has to be taken into account properly.

- The mass of the η is always taken as given by the Gell-Mann–Okubo relation, which reads

$$3M_\eta^2 = 2M_{K^\pm}^2 + 2M_{K^0}^2 - 2M_{\pi^\pm}^2 + M_{\pi^0}^2 \quad (28)$$

when taking into account isospin violation up to order e^2 and $m_u - m_d$. Deviations from this relation are beyond the accuracy considered in this paper, as the η -mass only enters via loop diagrams.

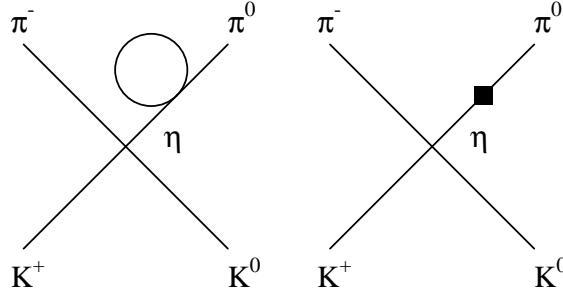


Figure 2: Diagrams contributing to $\pi^0\eta$ mixing at next-to-leading order. The labels “ π^0 ” and “ η ” refer to the tree-level mass eigenstates. The black square denotes a fourth-order insertion (strong or electromagnetic).

- $\pi^0\eta$ -mixing has to be taken into account at next-to-leading order. Details on how this is to be done can be found e.g. in [26, 27, 28, 29]. It is probably easiest to calculate the diagrams in fig. 2 directly in order to account for mixing beyond leading order. We have done the calculations using tree-level mass eigenfields for π^0 and η throughout. The off-diagonal element of the self-energy matrix (in the basis of tree-level eigenfields) may be written as $\Sigma_{\pi^0\eta}(q^2) = Z_{\pi^0\eta}q^2 + Y_{\pi^0\eta}$, such that $Z_{\pi^0\eta} = \partial\Sigma_{\pi^0\eta}/\partial q^2$ can be thought of as the off-diagonal analogy to the field renormalization factors. Denoting the tree-level amplitude for $\pi^-K^+ \rightarrow \eta K^0$ by T_η , we can write the additional mixing diagrams as

$$\begin{aligned} & T_\eta \times \frac{1}{M_{\pi^0}^2 - M_\eta^2} \times \Sigma_{\pi^0\eta}(q^2 = M_{\pi^0}^2) \\ = & T_\eta \times \underbrace{\left\{ \frac{Z_{\pi^0\eta}}{2} + \frac{1}{M_{\pi^0}^2 - M_\eta^2} \times \Sigma_{\pi^0\eta}\left(q^2 = \frac{1}{2}(M_{\pi^0}^2 + M_\eta^2)\right) \right\}}_{\epsilon^{(4)}}. \end{aligned} \quad (29)$$

$\epsilon^{(4)}$ thus defined is the correction to the tree level $\pi^0\eta$ mixing angle up to order $\mathcal{O}(q^4)$, as given e.g. in [29]. In contrast to the wave function renormalization factor $Z_{\pi^0\eta}$, $\epsilon^{(4)}$ is finite.

- When expressing the low-energy constant F in terms of physically observable decay constants, we always renormalize it such as to obtain F_π (as opposed to F_K , say). On tree level, the difference between using a normalization of the amplitude equal to $1/F_\pi^2$ and $1/F_\pi F_K$ amounts to nothing more but shifting certain contributions from tree to one-loop level, which makes no difference in the sum. However, it turns out

that the one-loop corrections e.g. for the scattering lengths are much smaller when normalizing the tree level expression to $1/F_\pi^2$, which means that in the seemingly more “symmetric” case of using $1/F_\pi F_K$, the bulk of the (large) corrections at $\mathcal{O}(q^4)$ have nothing to do with corrections to the scattering dynamics, but only with the renormalization of F_K .

For the one-loop contributions, the difference between F_π and F_K is of higher order, whereas the numerical difference is potentially significant (noting that these scale as $1/F^4$). Regarding $F_0 \simeq 88$ MeV [30] as the “natural” constant when writing down a scattering amplitude, F_π seems more appropriate than F_K .

Finally heavy-kaon ChPT, which we alluded to before already, also provides some insight on F_π versus F_K : there is of course no kaon decay constant in a kaon-number conserving theory, hence F_π is the only meson decay constant available. As heavy-kaon ChPT is supposed to have a better convergence behavior than SU(3) ChPT, but ultimately is equivalent up to matching of the different sets of LECs, it seems reasonable also from this perspective to only use F_π in the πK amplitudes.

- We use the charged pion decay constant in the absence of electromagnetism, as the value commonly used for the physical pion decay constant, $F_\pi = 92.4$ MeV [31], was extracted from *charged* pion decays with electromagnetic corrections already taken care of. The relation to the bare decay constant F is therefore as given in [15], and independent of photon loop effects or electromagnetic counterterms.

We display the isospin conserving and violating contributions, at tree and one-loop level, relative to the isospin symmetric tree level result (which we just denote by $a_0^{(2)}$ here for reasons of brevity). Numerically, these add up as follows:

$$\begin{aligned}
a_0^{(2)} &= -100.1 \times 10^{-3} / M_{\pi^\pm} , \\
a_0 &= a_0^{(2)} \left\{ 1 + \underbrace{0.006}_{\mathcal{O}(\epsilon)} + \underbrace{0.009}_{\mathcal{O}(\epsilon^2)} \right. \\
&\quad \left. + \underbrace{(0.121 \pm 0.009)}_{\mathcal{O}(p^4)} + \underbrace{(0.008 \pm 0.002)}_{\mathcal{O}(p^2\epsilon)} - \underbrace{(0.009 \pm 0.008)}_{\mathcal{O}(p^2\epsilon^2)} \right\} . \quad (30)
\end{aligned}$$

All errors quoted for the different contributions above are due to uncertainties in the respective strong and electromagnetic LECs as given in [17, 18]. The following comments are in order:

- The isospin symmetric corrections at one-loop order are moderate, given the expected slow convergence of chiral SU(3). As detailed above, this depends heavily on our choice to normalize the tree amplitude by $1/F_\pi^2$ and not $1/F_\pi F_K$. In fact, expanding the one-loop contributions in powers of M_π (equivalently to the heavy-kaon approach), one finds that they are suppressed essentially by a factor of M_π^2 (and not by $M_\pi M_K$ or M_K^2) compared to the tree level values, which is what one would expect from an SU(2) expansion and which accounts for the smallness of the one-loop corrections.

- Although they are very small corrections to the scattering length, one might worry about the fact that tree and one-loop level isospin breaking corrections (strong and electromagnetic effects taken separately) are of equal size. In order to understand the relative largeness of these effects, it is instructive to expand the terms given in app. A in powers of M_π . Isospin violating terms are suppressed in comparison to isospin conserving ones at the same chiral order by factors which happen to be small, but are of chiral order 1. On tree level, these suppression factors for $\pi^- K^+ \rightarrow \pi^0 K^0$ are ϵ and $e^2/M_\pi M_K$, respectively, see eq. (22). On one-loop level, however, where the isospin symmetric loop corrections are particularly small as discussed above, the isospin violating ones are suppressed with respect to these only by factors of $\epsilon M_K/M_\pi$ and $e^2 M_K/M_\pi^3$ (at leading order in M_π).

On the other hand, combining strong and electromagnetic isospin breaking effects, the corrections at one-loop level cancel to a large extent, leaving mainly an uncertainty due to a lack of sufficiently precise knowledge of the relevant counterterms. This cancellation does not take place at tree level. We have checked numerically that no significant errors arise from truncating the “exact” expressions at leading orders in the isospin breaking parameters ϵ , e^2 . In fact, the corrections arising thereof are at least one order of magnitude smaller than the accuracy displayed in eq. (30).

- With the large number of electromagnetic counterterms, one might have suspected that one cannot make any sensible prediction about electromagnetic effects at all. While the uncertainty quoted above is as large as the absolute size of the electromagnetic correction at one-loop level, it is, on the other hand, still not larger than the uncertainty stemming from our lack of knowledge of the values for the hadronic low-energy constants.

4.2 Infrared divergences and $\pi^- K^+ \rightarrow \pi^0 K^0 \gamma$

As mentioned in the previous section, photon loop corrections induce infrared divergences in the scattering amplitude. It is well known how to handle this problem, namely by introducing a small photon mass m_γ which brings the infrared divergences into a form $\sim \log m_\gamma$. Such terms enter both via wave function renormalization of charged mesons and via the loop function $G^{\pi K \gamma}(s)$, as discussed in app. B. One then has to include the corresponding radiative process ($\pi^- K^+ \rightarrow \pi^0 K^0 \gamma$ for the case in question) up to some maximal photon energy, given either by the maximal energy available due to kinematics, or by some experimental detector resolution ΔE below which soft photon radiation cannot be discriminated from the non-radiative process. We are interested in the threshold region, where the kinematical limit for the photon energy,

$$E_\gamma^{\max} = \frac{s - (M_{K^0} + M_{\pi^0})^2}{2\sqrt{s}}, \quad (31)$$

numerically amounts to 0.6 MeV, such that it seems reasonable to integrate the full cross section without making additional cuts on the photon energy. The infrared divergences cancel upon adding up the cross sections for both non-radiative and radiative processes. This is demonstrated in some detail in app. C.1.

We have emphasized in the previous chapter that the infrared divergences induced by photon loops vanish at threshold, such that one might even omit all these considerations when one is exclusively interested in the S–wave scattering length. The authors of [22] have argued, however, that one should rather *define* the S–wave scattering length from an infrared–finite quantity, which would be the combined total cross section. For an amplitude which can be expanded according to eq. (12), the total cross section at threshold is given in terms of the S–wave scattering length as

$$\sigma_{\text{thr}} = \frac{|\mathbf{q}_{\text{out}}|}{|\mathbf{q}_{\text{in}}|} 4\pi(a_0)^2 . \quad (32)$$

One may now replace the cross section on the left–hand side of eq. (32) by the combined total cross section $\sigma + \sigma^\gamma$ and define a_0 via eq. (32).

This is what was suggested in [22] for the similar case of the scattering process $\pi^+\pi^- \rightarrow \pi^0\pi^0(\gamma)$, where the authors claim to find a shift in the (redefined) scattering length induced by the (infrared–finite) remainder of the radiative cross section at threshold. We have however recalculated the cross section for $\pi^+\pi^- \rightarrow \pi^0\pi^0\gamma$ at threshold and find that it vanishes. This is in our opinion rather obvious for the isospin symmetric case, where the neutral pions in the final state are of the same mass as the charged incoming ones. One would therefore expect the corrections to the scattering length due to soft photon radiation to be small compared to other isospin breaking effects, as they should be suppressed by at least two powers in isospin breaking parameters (a factor e^2 in the cross section due to the photon coupling, and at least one power of the pion mass difference). The fact that this cross section vanishes exactly at threshold in the $\pi\pi$ case is due to the enhanced symmetry of this reaction, see app. C.2.

We do not find the cross section for $\pi^-K^+ \rightarrow \pi^0K^0\gamma$ to vanish exactly at threshold, but to be highly suppressed: the leading contribution is of order δ^4 in isospin breaking parameters, which is clearly way beyond the level of accuracy we achieve in our calculation of isospin breaking effects in the non–radiative amplitude. Details for the calculation can be found in app. C.2, the result found there is

$$\sigma_{\text{thr}}^\gamma = \frac{e^2}{105(2\pi)^3 F_\pi^4} \frac{|\mathbf{q}_{\text{out}}|}{|\mathbf{q}_{\text{in}}|} \frac{M_{K^\pm} M_{\pi^\pm}}{(M_{K^\pm} + M_{\pi^\pm})^3} (M_{K^\pm} - M_{K^0} + M_{\pi^\pm} - M_{\pi^0})^3 + \mathcal{O}(\delta^5) . \quad (33)$$

In addition to the high power in δ , there is even an unnatural suppression in the mass difference $(M_{K^\pm} - M_{K^0} + M_{\pi^\pm} - M_{\pi^0})$ which is due to a numerical cancellation of strong and electromagnetic isospin breaking effects. If one calculates a shift in the scattering length defined via eq. (32) which is due to the inclusion of the radiative cross section, $a_0 \rightarrow a_0 + a_0^\gamma$, the quantity a_0^γ is found to be

$$\begin{aligned} a_0^\gamma &= -\frac{e^2}{840\sqrt{2}\pi^3 F_\pi^2} \frac{(M_{K^\pm} - M_{K^0} + M_{\pi^\pm} - M_{\pi^0})^3}{(M_{K^\pm} + M_{\pi^\pm})^2} + \mathcal{O}(\delta^5) \\ &= -2.2 \times 10^{-14} / M_{\pi^\pm} = 2.2 \times 10^{-13} \times a_0^{(2)} , \end{aligned} \quad (34)$$

which is a suppression of about eleven orders of magnitude compared to the shifts in the scattering length calculated before. We therefore conclude that bremsstrahlung corrections are totally negligible for any analysis of $\pi\pi$ or πK bound state experiments.

4.3 S–wave effective range, P–wave scattering length

Although a precise knowledge of the S–wave scattering length is of highest interest for πK atom studies, one can of course also study isospin breaking corrections to other threshold parameters, particularly to the S–wave effective range b_0 and the P–wave scattering length a_1 . We will not show results for these in as much detail as for a_0 , but concentrate on the channel for which we have calculated the one–loop corrections to isospin breaking. We remark that, as indicated in eq. (27), photon loops also induce a term *linear* in $|\mathbf{q}_{\text{in}}|$ in the threshold expansion of the scattering amplitude, which we disregard here (as it can also be calculated and subtracted unambiguously).

The isospin symmetric tree level results for these two quantities are given by

$$b_0^{(2)} = -\sqrt{2} b_0^- = -\frac{M_K^2 + M_\pi^2}{8\sqrt{2}\pi F_\pi^2 M_\pi M_K (M_K + M_\pi)} , \quad (35)$$

$$a_1^{(2)} = -\sqrt{2} a_1^- = -\frac{1}{24\sqrt{2}\pi F_\pi^2 (M_K + M_\pi)} . \quad (36)$$

The isospin violating effects at tree level can then be expressed as

$$b_0(\pi^- K^+ \rightarrow \pi^0 K^0) = -\sqrt{2} b_0^- \left\{ 1 + \frac{\epsilon}{\sqrt{3}} - \frac{Z e^2 F_\pi^2}{M_K^2 + M_\pi^2} \right\} + \mathcal{O}(\delta^2) , \quad (37)$$

$$a_1(\pi^- K^+ \rightarrow \pi^0 K^0) = -\sqrt{2} a_1^- \left\{ 1 - \sqrt{3} \epsilon \right\} + \mathcal{O}(\delta^2) . \quad (38)$$

No electromagnetic effects affect the P–wave scattering length at this order.

We evaluate the fourth–order contributions to these threshold parameters numerically only, therefore we do not differentiate between strong and electromagnetic isospin violation at this level. Again, all corrections are given relative to the isospin symmetric tree–level result:

$$\begin{aligned} b_0^{(2)} &= -54.0 \times 10^{-3} / M_{\pi^\pm}^3 , \\ b_0 &= b_0^{(2)} \left\{ 1 + \underbrace{0.006}_{\mathcal{O}(\epsilon)} - \underbrace{0.002}_{\mathcal{O}(\epsilon^2)} + \underbrace{(0.012 \pm 0.038)}_{\mathcal{O}(p^4)} - \underbrace{(0.013 \pm 0.005)}_{\mathcal{O}(p^2\delta)} \right\} , \end{aligned} \quad (39)$$

$$\begin{aligned} a_1^{(2)} &= -4.7 \times 10^{-3} / M_{\pi^\pm}^3 , \\ a_1 &= a_1^{(2)} \left\{ 1 - \underbrace{0.02}_{\mathcal{O}(\epsilon)} + \underbrace{(0.53 \pm 0.14)}_{\mathcal{O}(p^4)} - \underbrace{(0.03 \pm 0.01)}_{\mathcal{O}(p^2\delta)} \right\} . \end{aligned} \quad (40)$$

We note that the isospin symmetric one–loop corrections to the P–wave scattering length are rather large compared to the leading term. The isospin breaking corrections for both quantities are of similar size as for a_0 , only slightly enhanced for a_1 . The main difference is that the cancellation between electromagnetic and $m_u - m_d$ effects at fourth order observed for a_0 does not occur here, such that isospin breaking at fourth chiral order is equally important as on tree level. If we compare the one–loop contributions only, the isospin breaking effects on the S–wave effective range appear to be very large, equally large even as the isospin symmetric one–loop corrections. However, as already hinted at by the error range for the latter, this does not result from an unnatural enhancement of isospin violation effects,

but from an accidental suppression of the isospin conserving part. Individual contributions to the latter (from separate loop diagrams, counterterms) are much larger.

In contrast to both the S–wave and the P–wave scattering lengths, the S–wave effective range as defined naively from the scattering amplitude alone is infrared divergent. The above results were achieved by setting m_γ equal to the maximal energy of a bremsstrahlung photon, which at threshold is roughly 0.6 MeV. This is what effectively happens when rendering infrared divergent expressions finite by including the appropriate radiative process, while we neglect here any finite contributions from the latter, see the discussion in the previous section. We also note that a redefinition of these higher–order threshold parameters from the infrared–finite total cross section (as done in the previous section for the S–wave scattering length) cannot be done unambiguously.

5 Summary

In this work, we have considered isospin violation in pion–kaon scattering near threshold. To systematically account for such effects due to the light quark mass difference as well as electromagnetic interactions, we have made use of SU(3) chiral perturbation theory in the presence of virtual photons. The pertinent results of this investigation can be summarized as follows:

- (1) Already at tree level, one has strong as well as electromagnetic isospin violation. We have considered all physical channels and found that these effects are in general small (at most two percent). In particular, the relative corrections are smaller than in the comparable case of $\pi\pi$ scattering where isospin violation at tree level is a purely electromagnetic effect. We have also stressed that considering one particular source of isospin violation only can ensue very misleading results.
- (2) Because of its relevance to the lifetime of πK atoms, we have considered the one–loop corrections to the S–wave scattering length for the process $\pi^- K^+ \rightarrow \pi^0 K^0$. The fourth–order isospin symmetric corrections are moderate and the isospin violation effects at this order cancel to a large extent (for the central values of the low–energy constants used here). The uncertainty in these isospin violating contributions is mainly due to the poor knowledge of the electromagnetic LECs K_i . This uncertainty is comparable to the one in the isospin symmetric amplitude induced by the variations in the strong LECs L_i .
- (3) We have also considered the radiative process $\pi^- K^+ \rightarrow \pi^0 K^0 \gamma$. We have explicitly demonstrated the cancellation of the infrared divergences. The remaining radiative cross section is strongly suppressed at threshold so that the properly redefined (finite) scattering length acquires no significant correction.
- (4) We have also given the one–loop corrections for the effective range b_0 and the P–wave scattering length a_1 for this channel. The isospin violating corrections are somewhat more pronounced than for the S–wave scattering length.

As pointed out in the introduction, for precisely predicting the $2P - 2S$ level shift in the πK atom, one would have to extend these considerations to the elastic scattering channel $\pi^- K^+ \rightarrow \pi^- K^+$ beyond the tree level result presented here.

After submission of this work, a similar analysis with comparable results has appeared, see [32].

We thank G. Ecker, A. Nehme, and P. Talavera for helping to resolve an error in the first version of the manuscript.

A S-wave scattering length at fourth order

In this appendix, we show the analytic expressions for the one-loop corrections to the scattering length a_0 for $\pi^- K^+ \rightarrow \pi^0 K^0$. The isospin violating effects are expanded up to order ϵ and e^2 . We express all these as relative corrections $\Delta^{(4)}a_0/a_0^{(2)}$. The low-energy constants with the infinite part subtracted are denoted by L_i^r , K_i^r , as done conventionally. Note however that we do not display the dependence of these various constants on the renormalization scale λ explicitly. All corrections given below are of course scale independent.

The isospin symmetric contribution is

$$\begin{aligned} \frac{\Delta_{\text{sym}}^{(4)}a_0}{a_0^{(2)}} &= \frac{M_\pi^2}{F_\pi^2} \left\{ 8L_5^r \right. \\ &- \frac{1}{16\pi^2} \left(\frac{1}{M_K^2 - M_\pi^2} \left[\left(4M_K^2 - \frac{5}{2}M_\pi^2 \right) \log \frac{M_\pi}{\lambda} - \frac{23}{9}M_K^2 \log \frac{M_K}{\lambda} + \left(\frac{14}{9}M_K^2 - \frac{M_\pi^2}{2} \right) \log \frac{M_\eta}{\lambda} \right] \right. \\ &+ \frac{4M_K}{9M_\pi} \left[\frac{\sqrt{(M_K - M_\pi)(2M_K + M_\pi)}}{M_K + M_\pi} \arctan \left(\frac{2(M_K + M_\pi)}{M_K - 2M_\pi} \sqrt{\frac{M_K - M_\pi}{2M_K + M_\pi}} \right) \right. \\ &\left. \left. - \frac{\sqrt{(M_K + M_\pi)(2M_K - M_\pi)}}{M_K - M_\pi} \arctan \left(\frac{2(M_K - M_\pi)}{M_K + 2M_\pi} \sqrt{\frac{M_K + M_\pi}{2M_K - M_\pi}} \right) \right] \right\}. \quad (41) \end{aligned}$$

The strong isospin violating part can be expressed as

$$\begin{aligned} \frac{\Delta_{\text{str}}^{(4)}a_0}{a_0^{(2)}} &= -\frac{\epsilon}{\sqrt{3}F_\pi^2} \left\{ 16M_\pi(M_K - M_\pi) L_3 + \frac{8(2M_K^4 - M_K^2 M_\pi^2 - 3M_K M_\pi^3 - M_\pi^4)}{3M_K M_\pi} L_5^r \right. \\ &\quad \left. - \frac{16(M_K^2 - M_\pi^2)(2M_K^2 + M_\pi^2)}{3M_K M_\pi} L_8^r \right. \\ &+ \frac{1}{16\pi^2} \left[\frac{72M_K^5 - 56M_K^4 M_\pi - 200M_K^3 M_\pi^2 + 21M_K^2 M_\pi^3 - 19M_K M_\pi^4 + 2M_\pi^5}{6M_K(M_K - M_\pi)^2(M_K + M_\pi)} M_\pi \log \frac{M_\pi}{\lambda} \right. \\ &- \frac{94M_K^4 - 185M_K^3 M_\pi - 915M_K^2 M_\pi^2 + 46M_K M_\pi^3 - 20M_\pi^4}{27(M_K - M_\pi)^2(M_K + M_\pi)} M_\pi \log \frac{M_K}{\lambda} \\ &\left. - \left(\frac{48M_K^7 - 48M_K^6 M_\pi + 388M_K^5 M_\pi^2 - 224M_K^4 M_\pi^3}{54M_K M_\pi(M_K - M_\pi)^2(M_K + M_\pi)} \right) \right] \end{aligned}$$

$$\begin{aligned}
& + \frac{192M_K^3M_\pi^4 + 259M_K^2M_\pi^5 - 269M_KM_\pi^6 - 6M_\pi^7}{54M_KM_\pi(M_K - M_\pi)^2(M_K + M_\pi)} \log \frac{M_\eta}{\lambda} \\
& + \frac{2M_\pi(16M_K^2 - 40M_KM_\pi - 47M_\pi^2)}{9(M_K - M_\pi)} \\
& - \frac{2M_KM_\pi(4M_K + M_\pi)}{3(M_K + M_\pi)} \sqrt{\frac{M_K - M_\pi}{2M_K + M_\pi}} \arctan \left(\frac{2(M_K + M_\pi)}{M_K - 2M_\pi} \sqrt{\frac{M_K - M_\pi}{2M_K + M_\pi}} \right) \\
& - \frac{2M_\pi(116M_K^4 - 79M_K^3M_\pi - 156M_K^2M_\pi^2 + 74M_KM_\pi^3 + 8M_\pi^4)}{27(M_K - M_\pi)^2(M_K + M_\pi)} \\
& \times \left. \left[\sqrt{\frac{M_K + M_\pi}{2M_K - M_\pi}} \arctan \left(\frac{2(M_K - M_\pi)}{M_K + 2M_\pi} \sqrt{\frac{M_K + M_\pi}{2M_K - M_\pi}} \right) \right] \right\}. \tag{42}
\end{aligned}$$

Finally, the electromagnetic corrections at one-loop level can be written as

$$\begin{aligned}
\frac{\Delta_{\text{em}}^{(4)} a_0}{a_0^{(2)}} & = e^2 \left\{ Z \left(8L_3 - \frac{4(2M_K - M_\pi)(2M_K + 7M_\pi)}{3M_KM_\pi} L_5^r \right) \right. \\
& - \frac{8}{3}(K_1^r + K_2^r) + \frac{6M_K^3 + 2M_K^2M_\pi - 6M_KM_\pi^2 + M_\pi^3}{6M_K(M_K^2 - M_\pi^2)} (2K_3^r - K_4^r) \\
& - \frac{M_K(4M_K^2 - 7M_\pi^2)}{9M_\pi(M_K^2 - M_\pi^2)} (K_5^r + K_6^r) - \frac{2}{9}(10K_5^r + K_6^r) \\
& \left. - \frac{M_\pi(2M_K^2 + M_\pi^2)}{9M_K(M_K^2 - M_\pi^2)} (K_9^r + K_{10}^r) + \frac{2(4M_K^2 - M_\pi^2)}{3M_KM_\pi} (K_{10}^r + K_{11}^r) \right\} \\
& + \frac{Ze^2}{16\pi^2} \left\{ \frac{40M_K^5 - 118M_K^4M_\pi + 22M_K^3M_\pi^2 + 26M_K^2M_\pi^3 - 71M_KM_\pi^4 + 11M_\pi^5}{6M_K(M_K - M_\pi)^3(M_K + M_\pi)} \log \frac{M_\pi}{\lambda} \right. \\
& - \frac{36M_K^5 - 97M_K^4M_\pi - 211M_K^3M_\pi^2 + 126M_K^2M_\pi^3 - 400M_KM_\pi^4 + 56M_\pi^5}{27M_\pi(M_K - M_\pi)^3(M_K + M_\pi)} \log \frac{M_K}{\lambda} \\
& - \frac{32M_K^5 + 296M_K^4M_\pi - 270M_K^3M_\pi^2 + 260M_K^2M_\pi^3 - 121M_KM_\pi^4 - 27M_\pi^5}{54M_K(M_K - M_\pi)^3(M_K + M_\pi)} \log \frac{M_\eta}{\lambda} \\
& + \frac{113M_K^4 - 138M_K^3M_\pi - 249M_K^2M_\pi^2 - 13M_KM_\pi^3 + 3M_\pi^4}{18M_K(M_K - M_\pi)^2(M_K + M_\pi)} \\
& - \frac{16M_K^2 - 17M_KM_\pi - 8M_\pi^2}{9(M_K + M_\pi)\sqrt{(2M_K + M_\pi)(M_K - M_\pi)}} \arctan \left(\frac{2(M_K + M_\pi)}{M_K - 2M_\pi} \sqrt{\frac{M_K - M_\pi}{2M_K + M_\pi}} \right) \\
& - \frac{32M_K^4 + 35M_K^3M_\pi - 108M_K^2M_\pi^2 - 40M_KM_\pi^3 + 44M_\pi^4}{27(M_K - M_\pi)^3\sqrt{(2M_K - M_\pi)(M_K + M_\pi)}} \\
& \quad \left. \times \arctan \left(\frac{2(M_K - M_\pi)}{M_K + 2M_\pi} \sqrt{\frac{M_K + M_\pi}{2M_K - M_\pi}} \right) \right\} \\
& - \frac{e^2}{16\pi^2} \left\{ \frac{12M_K^2 - 4M_KM_\pi - M_\pi^2}{2M_K(M_K + M_\pi)} \log \frac{M_\pi}{\lambda} + \frac{4M_K^2 + M_KM_\pi + 12M_\pi^2}{2M_\pi(M_K + M_\pi)} \log \frac{M_K}{\lambda} \right. \\
& \quad \left. - \frac{4M_K^2 - 18M_KM_\pi - M_\pi^2}{3M_KM_\pi} \right\}. \tag{43}
\end{aligned}$$

B Infrared divergent loop diagrams

The essential loop function containing an infrared divergence, stemming from the photon exchange diagram (a) in fig. 1, is

$$G^{\pi K\gamma}(s) = -i \int \frac{d^4k}{(2\pi)^4} \frac{1}{\left((q_\pi+k)^2 - M_{\pi^\pm}^2\right)\left((q_K-k)^2 - M_{K^\pm}^2\right)\left(k^2 - m_\gamma^2\right)}, \quad (44)$$

where $s = (q_K + q_\pi)^2$. Evaluating this in the kinematical region needed for the process in question, $s > (M_{K^\pm} + M_{\pi^\pm})^2$, we find

$$\begin{aligned} \text{Re } G^{\pi K\gamma}(s) &= \frac{1}{32\pi^2\sigma s} \left\{ \left[\log \sigma - \log\left(\frac{m_\gamma^2}{s}\right) \right] \left[\log \frac{1-z_1}{z_1} + \log \frac{z_2}{1-z_2} \right] \right. \\ &\quad + \frac{1}{2} \left[\log^2(1-z_1) - \log^2 z_1 + \log^2 z_2 - \log^2(1-z_2) \right] + \log \frac{z_2}{\sigma} \log \frac{z_1}{z_2} \\ &\quad \left. + \log \frac{1-z_1}{\sigma} \log \frac{1-z_2}{1-z_1} - 2 \left[\text{Li}\left(\frac{\sigma}{z_2}\right) + \text{Li}\left(\frac{\sigma}{1-z_1}\right) \right] - \frac{4\pi^2}{3} \right\} + \mathcal{O}(m_\gamma), \end{aligned} \quad (45)$$

$$\text{Im } G^{\pi K\gamma}(s) = \frac{1}{16\pi\sigma s} \left\{ \log\left(\frac{m_\gamma^2}{s}\right) - 2 \log \sigma \right\} + \mathcal{O}(m_\gamma), \quad (46)$$

where

$$\begin{aligned} z_{1/2} &= \frac{1}{2} \left(1 - \frac{\Delta}{s} \right) \mp \frac{\sigma}{2}, \quad \sigma = \sqrt{1 - \frac{2\Sigma}{s} + \frac{\Delta^2}{s^2}}, \\ \Sigma &= M_{K^\pm}^2 + M_{\pi^\pm}^2, \quad \Delta = M_{K^\pm}^2 - M_{\pi^\pm}^2, \end{aligned} \quad (47)$$

and

$$\text{Li}(z) = \int_1^z \frac{\log t}{1-t} dt \quad (48)$$

is the dilogarithm or Spence function. We have checked that this loop function coincides with the analogous one needed for $\pi\pi$ -scattering as given in [33, 22] when going to the limit of equal pion and kaon masses. Other infrared divergent loop contributions stem from the wave function renormalization of the charged pions (see e.g. [34]) and kaons,

$$\begin{aligned} Z_{\pi^\pm} &= -\frac{e^2}{4\pi^2} \log \frac{m_\gamma}{M_{\pi^\pm}} + \mathcal{O}(m_\gamma^0), \\ Z_{K^\pm} &= -\frac{e^2}{4\pi^2} \log \frac{m_\gamma}{M_{K^\pm}} + \mathcal{O}(m_\gamma^0). \end{aligned} \quad (49)$$

We write the tree level amplitude for $\pi^- K^+ \rightarrow \pi^0 K^0$ as

$$T^{(2)} = c_0 + c_s s + c_t t + c_u u, \quad (50)$$

where

$$\begin{aligned} c_0 &= \frac{B}{6\sqrt{2}F^2} \left((m_u - m_d) \cos \epsilon + (m_u + m_d - 2m_s) \frac{\sin \epsilon}{\sqrt{3}} \right) - \frac{Ze^2}{\sqrt{2}} \left(\cos \epsilon + \frac{\sin \epsilon}{\sqrt{3}} \right), \\ c_s &= -\frac{1}{2\sqrt{2}F^2} \left(\cos \epsilon + \frac{\sin \epsilon}{\sqrt{3}} \right), \quad c_t = \frac{\sin \epsilon}{\sqrt{6}F^2}, \quad c_u = \frac{1}{2\sqrt{2}F^2} \left(\cos \epsilon - \frac{\sin \epsilon}{\sqrt{3}} \right). \end{aligned} \quad (51)$$

The infrared divergent piece of the real part of the one-loop amplitude $T^{(4)}$ is then given by

$$\begin{aligned} (\text{Re } T^{(4)})^{\text{div}} &= T^{(2)} \times \frac{e^2}{8\pi^2} \left\{ \frac{s - \Sigma}{\sigma s} \left[\log \frac{1 - z_1}{z_1} + \log \frac{z_2}{1 - z_2} \right] \log \frac{m_\gamma}{\sqrt{s}} - \log \frac{m_\gamma}{M_{\pi^\pm}} - \log \frac{m_\gamma}{M_{K^\pm}} \right\} \\ &\equiv T^{(2)} \times \frac{e^2}{8\pi^2} L(m_\gamma). \end{aligned} \quad (52)$$

The total cross section is obtained from the amplitude via

$$\sigma = \frac{1}{64\pi^2 s} \frac{|\mathbf{q}_{\text{out}}|}{|\mathbf{q}_{\text{in}}|} \int |T|^2 d\Omega, \quad (53)$$

with $|\mathbf{q}_{\text{in}}|$ and $|\mathbf{q}_{\text{out}}|$ defined as in eqs. (10), (11). The infrared divergent part of the total cross section can be calculated from eq. (53) to be

$$\begin{aligned} \sigma^{\text{div}} &= \frac{e^2}{(4\pi)^3} \frac{|\mathbf{q}_{\text{out}}|}{|\mathbf{q}_{\text{in}}| s} \left\{ \left[c_0 + \left(c_s - \frac{c_t + c_u}{2} \right) s + \frac{c_t + c_u}{2} (M_{K^\pm}^2 + M_{K^0}^2 + M_{\pi^\pm}^2 + M_{\pi^0}^2) \right. \right. \\ &\quad \left. \left. - \frac{c_t - c_u}{2} \frac{(M_{K^\pm}^2 - M_{\pi^\pm}^2)(M_{K^0}^2 - M_{\pi^0}^2)}{s} \right]^2 + \frac{4}{3} (c_t - c_u)^2 |\mathbf{q}_{\text{in}}|^2 |\mathbf{q}_{\text{out}}|^2 \right\} L(m_\gamma). \end{aligned} \quad (54)$$

C The radiative cross section

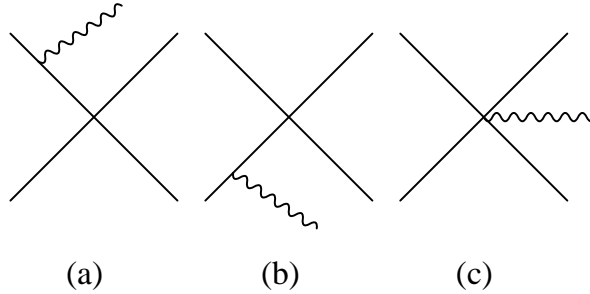


Figure 3: Diagrams contributing to $\pi^- K^+ \rightarrow \pi^0 K^0 \gamma$ at tree level.

The amplitude for the process

$$\pi^-(q_\pi) K^+(q_K) \rightarrow \pi^0(p_\pi) K^0(p_K) \gamma(l) \quad (55)$$

is given, to lowest order, by

$$\begin{aligned} T^\gamma &= \frac{e \epsilon^* \cdot (2q_K - l)}{2q_K \cdot l - m_\gamma^2} (c_0 + c_s s_2 + c_t t_\pi + c_u u_\pi) \\ &- \frac{e \epsilon^* \cdot (2q_\pi - l)}{2q_\pi \cdot l - m_\gamma^2} (c_0 + c_s s_2 + c_t t_K + c_u u_K) \\ &+ \frac{e}{2\sqrt{2}F^2} \epsilon^* \cdot \left\{ (q_K - q_\pi + p_K - p_\pi) \cos \epsilon + (q_K - q_\pi - 3p_K + 3p_\pi) \frac{\sin \epsilon}{\sqrt{3}} \right\}, \end{aligned} \quad (56)$$

where

$$s_2 = (p_\pi + p_K)^2, \quad t_{\pi/K} = (q_{\pi/K} - p_{\pi/K})^2, \quad u_{\pi/K} = (q_{\pi/K} - p_{K/\pi})^2. \quad (57)$$

The three terms in eq. (56) correspond to the three diagrams in fig. 3. The total cross section can be calculated from this amplitude by

$$\sigma^\gamma = \frac{1}{(2\pi)^5} \frac{1}{4|\mathbf{q}_{\text{in}}|\sqrt{s}} \int dE_l \int d\Omega_{p_\pi} \int d\Omega_{p_{\pi l}} \frac{|\mathbf{p}_\pi||\mathbf{l}|}{8 \left(E_{K^0} + E_{\pi^0} \left(1 + \frac{|\mathbf{l}|}{|\mathbf{p}_\pi|} \cos \theta_{p_{\pi l}} \right) \right)} |T^\gamma|^2, \quad (58)$$

where θ_{p_π} refers to the the angle between the outgoing pion and the axis of the incoming particles (in their center-of-mass system), and $\theta_{p_{\pi l}}$ denotes the relative angle between the outgoing pion and the photon.

C.1 Infrared divergence

One important check resulting from the exact calculation of the radiative cross section is that the infrared divergences indeed cancel when combining radiative and non-radiative cross sections, we therefore demonstrate how to isolate the infrared divergent parts in the cross section eq. (58). These stem exclusively from the lower integration bound of the E_l -integration, therefore it suffices to collect the leading powers in $1/E_l$ of the integrand. The squared matrix element simplifies considerably in this approximation, one may set $s_2 \rightarrow s$, $t_{\pi/K} \rightarrow t$, $u_{\pi/K} \rightarrow u$, and obtains

$$|T^\gamma|^2 = e^2 \left\{ -\frac{M_{\pi^\pm}^2}{(l \cdot q_\pi)^2} - \frac{M_{K^\pm}^2}{(l \cdot q_K)^2} + \frac{s - M_{\pi^\pm}^2 - M_{K^\pm}^2}{l \cdot q_\pi l \cdot q_K} \right\} (c_0 + c_s s + c_t t + c_u u)^2 + \mathcal{O}(E_l^{-1}). \quad (59)$$

As is well known from Quantum Electrodynamics, infrared divergences arise only from diagrams with soft photon radiation *from external legs* (diagrams (a), (b) in fig. 3), and indeed contributions from the diagram where the photon is radiated from the πK -vertex (diagram (c) in fig. 3) play no role here. Furthermore, we can set $|\mathbf{p}_\pi| = |\mathbf{q}_{\text{out}}|$ (which is, as above, the modulus of the outgoing momentum of the *non-radiative* process), and use the abbreviations $y = \cos \theta_{p_{\pi l}}$, $z = \cos \theta_{p_\pi}$, to obtain

$$\begin{aligned} \sigma^\gamma &= \frac{e^2}{(4\pi)^3} \frac{|\mathbf{q}_{\text{out}}|}{4|\mathbf{q}_{\text{in}}|s} \int_{m_\gamma}^{E_\gamma^{\text{max}}} dE_l E_l \int_{-1}^1 dz \int_{-1}^1 dy \int_0^{2\pi} \frac{d\phi_{p_{\pi l}}}{2\pi} \\ &\times \left\{ -\frac{M_{\pi^\pm}^2}{(l \cdot q_\pi)^2} - \frac{M_{K^\pm}^2}{(l \cdot q_K)^2} + \frac{s - M_{\pi^\pm}^2 - M_{K^\pm}^2}{l \cdot q_\pi l \cdot q_K} \right\} (c_0 + c_s s + c_t t + c_u u)^2 + \mathcal{O}(m_\gamma^0). \quad (60) \end{aligned}$$

Note that in this approximation, the term $c_0 + c_s s + c_t t + c_u u$ depends, of all integration variables, only on z (via t and u). The $\phi_{p_{\pi l}}$ integration is relatively straightforward when using

$$l \cdot q_{\pi/K} = E_l |\mathbf{q}_{\text{in}}| \left(S_{\pi/K} \mp \cos \alpha \right), \quad (61)$$

where

$$S_{\pi/K} = \frac{s \mp M_{K^\pm}^2 \pm M_{\pi^\pm}^2}{2|\mathbf{q}_{\text{in}}|\sqrt{s}}, \quad \cos \alpha = yz - \sqrt{1-y^2}\sqrt{1-z^2} \cos \phi_{p_{\pi l}}, \quad (62)$$

such that, for example, the first term in the curly brackets in eq. (60) yields

$$M_{\pi^\pm}^2 \int_{-1}^1 dy \int_0^{2\pi} \frac{d\phi_{p\pi l}}{2\pi} \frac{1}{(l \cdot q_\pi)^2} = \frac{M_{\pi^\pm}^2}{E_l^2 |\mathbf{q}_{\text{in}}|^2} \int_{-1}^1 dy \frac{S_\pi - yz}{(S_\pi^2 - 1 - 2S_\pi yz + y^2 + z^2)^{3/2}} = \frac{2}{E_l^2}, \quad (63)$$

and the other terms can be evaluated similarly. The only remaining z -dependence is the one which is also inherent in the integration of the non-radiative cross section,

$$\int_{-1}^1 dz (c_0 + c_s s + c_t t + c_u u)^2. \quad (64)$$

Altogether, one ends up with

$$\begin{aligned} \sigma^\gamma &= \frac{e^2}{(4\pi)^3} \frac{|\mathbf{q}_{\text{out}}|}{|\mathbf{q}_{\text{in}}|s} \log\left(\frac{E_\gamma^{\text{max}}}{m_\gamma}\right) \left\{ \frac{s - M_{K^\pm}^2 - M_{\pi^\pm}^2}{2|\mathbf{q}_{\text{in}}|\sqrt{s}} \left(\log \frac{S_K + 1}{S_K - 1} + \log \frac{S_\pi + 1}{S_\pi - 1} \right) - 2 \right\} \\ &\times \left\{ \left[c_0 + \left(c_s - \frac{c_t + c_u}{2} \right) s + \frac{c_t + c_u}{2} (M_{K^\pm}^2 + M_{K^0}^2 + M_{\pi^\pm}^2 + M_{\pi^0}^2) \right. \right. \\ &\quad \left. \left. - \frac{c_t - c_u}{2} \frac{(M_{K^\pm}^2 - M_{\pi^\pm}^2)(M_{K^0}^2 - M_{\pi^0}^2)}{s} \right]^2 + \frac{4}{3} (c_t - c_u)^2 |\mathbf{q}_{\text{in}}|^2 |\mathbf{q}_{\text{out}}|^2 \right\} + \mathcal{O}(m_\gamma^0), \end{aligned} \quad (65)$$

which cancels the m_γ -divergence in eq. (54).

C.2 The radiative cross section at threshold

The other aspect of the radiative cross section on which one would like to have analytical information is the remainder at threshold. As the incoming charged particles are at rest at threshold, the angular integration for the total cross section simplifies considerably: the integration $d\Omega_{p\pi}$ is trivial, and so is the integration $d\phi_{p\pi l}$, hence the only angular variable to integrate is $dy = d\cos\theta_{p\pi l}$, which is most conveniently done in the center-of-mass frame of the outgoing $\pi^0 K^0$ system. Large cancellations take place, such that one obtains a surprisingly simple expression:

$$\begin{aligned} \int_{-1}^1 dy |T^\gamma|_{\text{thr}}^2 &= \frac{e^2}{24F^4} (\cos\epsilon - \sqrt{3}\sin\epsilon)^2 \frac{(M_{K^\pm} + M_{\pi^\pm})^2}{M_{K^\pm} M_{\pi^\pm}} \\ &\times \frac{(s_2 - (M_{K^\pm} - M_{\pi^\pm})^2)(s_2 - (M_{K^0} - M_{\pi^0})^2)(s_2 - (M_{K^0} + M_{\pi^0})^2)}{s_2^2}. \end{aligned} \quad (66)$$

In order to obtain eq. (66), it is essential to take the radiation from the four-meson vertex (diagram (c) in fig. 3) into account, the vertex of which is linked to the $\pi^- K^+ \rightarrow \pi^0 K^0$ vertex by gauge symmetry. In fact, we find that just by expressing the coefficients for the 5-point vertex (the third term in eq. (56)) by c_t and c_u , any dependence on c_0 and c_s drops out completely. This is why for the case of $\pi^+ \pi^- \rightarrow \pi^0 \pi^0 \gamma$, the cross section vanishes at threshold: the lowest-order $\pi^+ \pi^- \rightarrow \pi^0 \pi^0$ vertex is proportional to $s - M_{\pi^0}^2$ (in the σ gauge), and the $\pi^+ \pi^- \rightarrow \pi^0 \pi^0 \gamma$ point vertex vanishes (again in the σ gauge). Furthermore, the result of eq. (66) is proportional to $(c_t - c_u)^2$ which demonstrates that only the particular ‘‘asymmetry’’ of the reaction in question allows a finite remainder to survive at threshold.

Transforming the remaining integration over the energy of the outgoing photon into an integration of s_2 , we obtain the total cross section at threshold via

$$\sigma_{\text{thr}}^\gamma = \frac{1}{(8\pi)^3} \frac{|\mathbf{q}_{\text{out}}|}{|\mathbf{q}_{\text{in}}|s} \int_{s_2^{\text{thr}}}^s ds_2 \left(\frac{s-s_2}{s_2} \right) \sqrt{\frac{(s_2 - (M_{K^0} - M_{\pi^0})^2)(s_2 - (M_{K^0} + M_{\pi^0})^2)}{(s - (M_{K^0} - M_{\pi^0})^2)(s - (M_{K^0} + M_{\pi^0})^2)}} \times \int_{-1}^1 dy |T^\gamma|_{\text{thr}}^2, \quad (67)$$

where $s_2^{\text{thr}} = (M_{K^0} + M_{\pi^0})^2$ is the minimal energy (squared) for the final $\pi^0 K^0$ system. Eq. (67) is evaluated to leading order in isospin violation parameters, yielding the result

$$\sigma_{\text{thr}}^\gamma = \frac{e^2}{105(2\pi)^3 F_\pi^4} \frac{|\mathbf{q}_{\text{out}}|}{|\mathbf{q}_{\text{in}}|s} \frac{M_{K^\pm} M_{\pi^\pm}}{M_{K^\pm} + M_{\pi^\pm}} \left(M_{K^\pm} - M_{K^0} + M_{\pi^\pm} - M_{\pi^0} \right)^3 + \mathcal{O}(\delta^5). \quad (68)$$

In terms of fundamental isospin breaking parameters, the meson mass difference in eq. (68) can be expressed as

$$M_{K^\pm} - M_{K^0} + M_{\pi^\pm} - M_{\pi^0} = \frac{B(m_u - m_d)}{2M_K} + Ze^2 F^2 \left(\frac{1}{M_K} + \frac{1}{M_\pi} \right) + \mathcal{O}(\delta^2). \quad (69)$$

References

- [1] G. Colangelo, J. Gasser, and H. Leutwyler, Phys. Lett. B488 (2000) 261.
- [2] M. Zeller (for the BNL E865 Collaboration), “New Measurement of the Properties of K_{e4}^+ Decays”, talk given at April Meeting of the American Physical Society, Washington, D.C., April 28 – May 1, 2001.
- [3] B. Adeva et al., CERN-SPSLC-95-1, CERN-SPSLC-P-284, Dec 1994.
- [4] C.G. Callan and I. Klebanov, Nucl. Phys. B262 (1985) 365.
- [5] A. Roessl, Nucl. Phys. B555 (1999) 507.
- [6] S.M. Ouellette, hep-ph/0101055.
- [7] S. Descotes, L. Girlanda, and J. Stern, JHEP 0001 (2000) 041; S. Descotes and J. Stern, Phys. Lett. B488 (2000) 274; S. Descotes, JHEP 0103 (2001) 002.
- [8] V. Bernard, N. Kaiser, and U.-G. Meißner, Phys. Rev. D43 (1991) R2757.
- [9] B. Ananthanarayan and P. Büttiker, Eur. Phys. J. C19 (2001) 517.
- [10] B. Adeva et al., CERN-SPSC-2000-032, CERN-SPSC-P-284-ADD-1, Aug 2000.
- [11] H.-Ch. Schröder et al., Phys. Lett. B469 (1999) 25.
- [12] A. Gall, J. Gasser, V.E. Lyubovitskij, and A. Rusetsky, Phys. Lett. B462 (1999) 335; J. Gasser, V.E. Lyubovitskij, and A. Rusetsky, Phys. Lett. B471 (1999) 244; J. Gasser, V.E. Lyubovitskij, A. Rusetsky, and A. Gall, Phys. Rev. D64 (2001) 016008.
- [13] H. Jallouli and H. Sazdjian, Phys. Rev. D58 (1998) 014011; (E) *ibid* D58 (1998) 099901.
- [14] V. Bernard, N. Kaiser, and U.-G. Meißner, Nucl. Phys. B357 (1991) 129.
- [15] J. Gasser and H. Leutwyler, Nucl. Phys. B250 (1985) 465.
- [16] R. Urech, Nucl. Phys. B433 (1995) 234.

- [17] J. Bijnens, G. Ecker, and J. Gasser, in: L. Maiani, G. Pancheri, and N. Paver (Eds.), *The second DAΦNE Physics Handbook* (INFN, Frascati) (1995).
- [18] R. Baur and R. Urech, Nucl. Phys. B499 (1997) 319.
- [19] S. Weinberg, Phys. Rev. Lett. 17 (1966) 616.
- [20] R.W. Griffith, Phys. Rev. 176 (1968) 1705.
- [21] U.-G. Meißner, G. Müller, and S. Steininger, Phys. Lett. B406 (1997) 154.
- [22] M. Knecht and R. Urech, Nucl. Phys. B519 (1998) 329.
- [23] F.S. Roig and A.R. Swift, Nucl. Phys. B104 (1976) 533.
- [24] S. Weinberg, Trans. New York Acad. Sci. 38 (1977) 185.
- [25] U.-G. Meißner and S. Steininger, Phys. Lett. B419 (1998) 403.
- [26] J. Gasser and H. Leutwyler, Nucl. Phys. B250 (1985) 539.
- [27] H. Neufeld and H. Rupertsberger, Z. Phys. C68 (1995) 91.
- [28] G. Amoros, J. Bijnens, and P. Talavera, Nucl. Phys. B602 (2001) 87.
- [29] G. Ecker, G. Müller, H. Neufeld, and A. Pich, Phys. Lett. B477 (2000) 88.
- [30] J. Gasser and H. Leutwyler, Phys. Lett. B125 (1983) 325; Ann. Phys. (NY) 158 (1984) 142.
- [31] B.R. Holstein, Phys. Lett. B244 (1990) 83.
- [32] A. Nehme and P. Talavera, hep-ph/0107299.
- [33] M. Wicky, Diploma Thesis, University of Bern (1996), unpublished.
- [34] B. Kubis and U.-G. Meißner, Nucl. Phys. A671 (2000) 332.